Planta (2025) 262:102
https://doi.org/10.1007/s00425-025-04819-6

ORIGINAL ARTICLE

Gamma radiation-induced molecular toxicity and effects on pluripotent stem cells of the radiosensitive conifer Norway spruce (*Picea abies*)

Payel Bhattacharjee[1,2] · YeonKyeong Lee[1,2,3] · Marcos Viejo[1,4,5] · Gareth B. Gillard[6] · Simen Rød Sandve[6] · Torgeir R. Hvidsten[7] · Brit Salbu[2,8] · Dag A. Brede[2,8] · Jorunn E. Olsen[1,2]

Received: 27 May 2025 / Accepted: 2 September 2025 / Published online: 17 September 2025

Main conclusion

Regardless of DNA- and organelle damage and huge transcriptomic shifts towards stress management pathways after gamma irradiation at 1–100 mGy h^{-1}, pluripotent stem cells of Norway spruce were able to retain their stemness.

Abstract

Conifers are among the most radiosensitive plant species. Elevated, sublethal levels of ionising radiation result in reduced apical dominance in conifers, indicating a negative effect on shoot apical meristems (SAMs). The SAMs, harbouring the pluripotent stem cells, generate all the cells of the shoot, enabling growth and reproduction. However, knowledge on the effects of ionising radiation on such stem cells is scarce, but important for risk assessment and radioprotection of plants in contaminated ecosystems. Here, we assessed the sensitivity of in vitro-grown stem cells of Norway spruce to 144 h of gamma irradiation at 1–100 mGy h^{-1}, using such cells as a model for molecular toxicity of gamma radiation in conifers. Although there were no visible effects of the gamma irradiation on cell proliferation and subsequent embryo formation, dose rate-dependent DNA damage was observed at $\geq$ 10 mGy h^{-1}, and comprehensive organelle damage at all dose rates. Massive dose rate-dependent transcriptome changes occurred, with downregulation of a range of genes related to cell division, DNA repair and protein folding but upregulation of stress-related hormonal pathways and several antioxidant-related genes. The upregulation of such genes, survival and continued proliferation of at least a subset of cells and the post-irradiation normalisation of expression of DNA repair and protein-folding genes together with somatic embryo formation suggest that stem cells are able to recover from gamma-irradiation-induced stress. Collectively, regardless of cellular abnormalities after

Communicated by Dorothea Bartels.

Payel Bhattacharjee and YeonKyeong Lee—equal contribution.

✉ Jorunn E. Olsen
jorunn.olsen@nmbu.no

Payel Bhattacharjee
payel.bhattacharjee@nmbu.no

[1] Department of Plant Sciences, Faculty of Biosciences, Norwegian University of Life Sciences, P.O. Box 5003, N-1432 Ås, Norway

[2] Centre of Environmental Radiation (CERAD), Norwegian University of Life Sciences, P.O. Box 5003, N-1432 Ås, Norway

[3] Department of Plant Biotechnology, Korea University Graduate School, 145 Anam-Ro, 17 Seongbuk-Ku, Seoul, Republic of Korea

[4] Institute of Bioeconomy (NIBIO), P.O. Box 115, N-1431 Ås, Norway

[5] Department of Functional Biology, University of Santiago de Compostela, Santiago de Compostela, Spain

[6] Centre of Integrative Genetics, Department of Animal Sciences, Faculty of Biosciences, Norwegian University of Life Sciences, P.O. Box 5003, N-1432 Ås, Norway

[7] Faculty of Chemistry, Biotechnology and Food Science, Norwegian University of Life Sciences, P.O. Box 5003, N-1432 Ås, Norway

[8] Faculty of Environmental Sciences and Natural Resource Management, Norwegian University of Life Sciences, P.O. Box 5003, N-1432 Ås, Norway

gamma irradiation, and huge transcriptomic shifts towards stress management pathways, the pluripotent stem cell cultures were able to retain their stemness.

Keywords DNA damage · Gene expression · Ionising radiation · Organelle damage · Somatic embryogenesis · Transcriptome

Abbreviations

DEG Differentially expressed gene
DDR DNA damage repair
SAM Shoot apical meristem
UPR Unfolded protein response

Introduction

The extremely high ionising radiation doses from radioactive particles released from the Chernobyl nuclear power plant (ChNPP) accident on 26th April 1986 resulted in massive mortality of the conifer tree species Scots pine (*Pinus sylvestris* L.) in a nearby 4.5 km^2 forest area (Kashparova et al. 2020). In addition, elevated, sublethal radiation in the Chernobyl surroundings and in the Fukushima nuclear power plant accident area (2011, Japan) resulted in needle chlorosis, necrosis, and reduced apical dominance leading to a bushy appearance in conifer trees such as Scots pine (*Pinus sylvestris* L.), Norway spruce (*Picea abies* L. (H). Karst), Japanese red pine (*Pinus densiflora* Sieb. et Zucc.) and Japanese fir (*Abies firma* Sieb. et Zucc.) (Geraskin et al. 2008; Watanabe et al. 2015; Yoschenko et al. 2016; Kashparova et al. 2020). The reduced apical dominance implies a negative effect on the shoot apical meristems (SAMs). After more than three decades, in 2018, Scots pine trees in sites with elevated radiation near the ChNPP still showed reduced apical dominance and increased DNA damage in shoot tips compared to trees grown in sites with background radiation (Nybakken et al. 2023).

The SAM and the root apical meristem (RAM), which are laid down during embryogenesis, harbour the pluripotent stem cells that continuously generate cells forming vegetative organs under permissive environmental conditions and retain their stemness throughout the life of the plant (Umeda et al. 2021). The stem cells of the SAM also generate the reproductive meristems that are the source of the female and male gametophytes, which eventually contribute to the formation of embryos after fertilisation. The high mutation rates in Scots pine progeny growing under chronic ionising radiation in the Chernobyl area (Caplin and Willey 2018) support adverse effects on the pluripotent cells of the SAMs, the reproductive meristems and embryo development. However, detailed information about the radiosensitivity of plant stem cells and the effect on their stemness is limited.

Conifers are among the most radiosensitive plant species, while grasses and *Arabidopsis thaliana* are highly tolerant (Sparrow and Miksche 1961; Barescut et al. 2011; Blagojevic et al. 2019a, b; Bhattacharjee et al. 2025). Under laboratory conditions, gamma irradiation experiments employing up to 540 mGy h^{-1} from a ^{60}Co source for 144 h resulted in growth inhibition in Norway spruce and Scots pine seedlings at ≥ 20–40 mGy h^{-1}, more disorganised SAMs with increasing dose rate, and mortality at the highest dose rates (Blagojevic et al. 2019a). By contrast, only a slight delay in lateral root formation and flower bud appearance at dose rates ≥ 290–400 mGy h^{-1} was observed in *A. thaliana*, with no visible negative effects on the SAMs, and no mortality. Moreover, significant DNA damage was observed in all three species exposed to dose rates from 1 mGy h^{-1}, but with more DNA damage in the conifers than in *A. thaliana* (Blagojevic et al. 2019a).

Ionising radiation can result in damage to vital cellular macromolecules such as nucleic acids, lipids, and proteins through direct ionisation and the formation of reactive oxygen species (ROS) (You and Chan 2015). Several studies, particularly in *A. thaliana*, have indicated the activation of DNA damage repair (DDR) and antioxidants protecting against oxidative stress in plants during exposure to ionising radiation (Kim et al. 2019). The DDR encompasses a complex cascade of events including checkpoint activation, cell cycle arrest or endoreduplication, activation of different DDR pathways, and programmed cell death (PCD). A recent comparative study suggested more efficient transcriptional mobilisation of DDR and antioxidants in gamma-irradiated seedlings of *A. thaliana* than Norway spruce (Bhattacharjee et al. 2025). However, despite that stem cells in the SAMs and RAMs are crucial for vegetative and reproductive plant development in natural and man-made ecosystems, the effect of ionising radiation on repair and protection systems in stem cells has previously not been investigated. Additionally, stressful conditions typically lead to the stiffening of the plant cell wall through interaction between stress-induced ROS formation, cell wall integrity sensing, and hormone signalling pathways (Tenhaken 2014; Novaković et al. 2018). However, the knowledge of how ionising radiation affects the plant cell wall composition is limited.

A powerful model system for pluripotent stem cells of conifers can be induced in vitro from e.g., excised zygotic embryos or primordial shoot explants (Varis et al. 2018). Such stem cells can retain their stemness for a very long time and generate somatic embryos upon induction treatment, rendering it a valuable tool to study embryogenesis in plants with long generation times such as conifers, e.g., about 25 years in Norway spruce.

In this study, in vitro-grown pluripotent stem cells of Norway spruce were employed to analyse radiotoxicity in ecologically and economically important conifers, and specifically to test the hypothesis that low to moderate levels of ionising radiation affect the viability and stemness of stem cells in conifers. Given the importance of the stem cell-harbouring apical meristems for growth, reproduction and survival of plants, such information is important for predicting responses of ionising radiation in ecosystems, and accordingly for risk assessments and radioprotection. Here, stem cells of Norway spruce were gamma-irradiated and the damage and repair mechanisms as well as effects associated with the molecular cell physiology were investigated.

Materials and methods

Plant materials and pre-growing conditions

In vitro stem cell cultures of Norway spruce (*Picea abies* (L.) H. Karst.) were generated following the protocol by Kvaalen and Johnsen (2008). This included the following steps: A single zygotic seed originating from controlled crosses of the parents #26509 and #2707 (Johnsen et al. 2005) was used to initiate cultures of genetically identical cells (pluripotent stem cells) denoted as clone B10V. Cell proliferation media (PM) with the following composition was used: AL medium (formulated as a basal medium for in vitro culture of *Abies lasiocarpa*) (Kvaalen et al. 2005) supplemented with inositol (10%, w/v), a revised vitamin mixture previously used for in vitro culture of Douglas-fir cotyledons (Gupta and Durzan 1985), 2,4 dichlorophenoxy acetic acid (2,4-D; 10 µM), benzyl aminopurine (BAP; 5 µM), sucrose (1%, w/v), and Phytagel (P-8169; Sigma-Aldrich,; 0.3% w/v) (Yakovlev et al. 2014). The proliferating cells were kept as cell aggregates on PM in Petri dishes of 9 cm diameter at 23 °C in darkness. The cell aggregates (10 per dish) were divided and transferred to fresh media every two weeks until an adequate number of aggregates was obtained for the gamma irradiation experiments.

Table 1 The gamma radiation treatments applied in the experiments with exposure of stem cells of Norway spruce for 144 h using a ^{60}Co source

Dose rate (mGy h^{-1})	Dose rate interval (mGy h^{-1})		Total dose (mGy)
	Min	Max	
0	0.002	0.006	0
1	1.0	1.1	144
10	10.5	10.6	1440
20	18.7	21.0	2880
40	33.3	43.9	5760
100	83.8	114.8	14,400

Gamma irradiation of stem cells and growing conditions during the irradiation

The FIGARO low dose gamma irradiation facility (^{60}Co; 1173.2 and 1332.5 keV γ-rays) at the Norwegian University of Life Sciences (Lind et al. 2019) was used to expose aggregates of proliferating stem cells on PM to gamma radiation at 1, 10, 20, 40, and 100 mGy h^{-1} for 144 h (6 days) in the dark at 23 °C ± 1 °C. To obtain these dose rates, the Petri dishes containing densely spaced, not overlapping cell aggregates were placed at different distances from the ^{60}Co source and rotated 180° halfway through the experiment to ensure that all cells received as even gamma radiation as possible. The dose rates to water and dose rate intervals (Table 1) were calculated from the air kerma rates according to Hansen et al. (2019) as previously described (Blagojevic et al. 2019a, b). Two Petri dishes containing 10–15 cell aggregates each per dose rate were exposed in each of two repeated experiments, with unexposed control samples kept in the same room outside the radiation sector, behind lead shields. Thus, per dose rate, altogether 40 or more cell aggregates were exposed.

Post-irradiation growing conditions

To evaluate the post-irradiation cell proliferation, gamma-irradiated cell aggregates were maintained in the proliferation media (PM) at 23 °C in darkness for 7 weeks with change of media and division of the cell aggregates every two weeks. Proliferation stage 1 (P1) and 2 (P2) denote the stages 5 and 7 weeks on PM after the gamma irradiation, respectively. Thereafter, to study the after-effects of the gamma irradiation on subsequent embryogenesis, cell aggregates were transferred to maturation media (MM), consisting of PM without the growth regulators 2,4-D and BAP, but MM1 was supplemented with 20 µM abscisic acid (ABA; A8451, Sigma-Aldrich) and 2 µM indole butyric acid (IBA; Sigma-Aldrich). The subsequent MMs (MM2 and MM3) were supplemented only with ABA (20 uM) and not IBA. The carbon source was changed from sucrose to

maltose and the medium was supplemented with polyethylene glycol (PEG4000; Fluka) (5%, 10% and 13% w/v in MM in stage 1, 2 and 3, respectively) (Yakovlev et al. 2014). The cell aggregates were transferred to fresh MM every two weeks. Maturation stage 1 and 2 denote the stages 11 and 15 weeks after the gamma irradiation, respectively, corresponding to 4 and 8 weeks after the transfer to MM. Maturation stage 3–1, 3–2 and 3–3 denote the stages 17, 20 and 24 weeks after the gamma exposure, corresponding to 10, 13 and 17 weeks on MM.

COMET assay for analysis of DNA damage

To quantify the DNA damage after gamma irradiation, the COMET assay was used following the protocol of Gichner (2003) with some modifications as described by Blagojevic et al. (2019a). To avoid light-induced DNA damage, the assay was performed under inactinic red-light conditions. Briefly, the protocol included isolation of cell nuclei from approximately 200 mg cells per treatment and electrophoresis in agarose gels under alkaline pH, followed by quantification of the DNA in the COMET tail (elongated cell nuclei due to DNA damage) using fluorescence microscopy. Per gamma dose rate, three repeated samples with 65–70 nuclei per sample were investigated individually for DNA damage using three gels per sample. The median value for each sample was calculated, followed by calculation of the average value for the three repeated samples, according to (Koppen et al. 2017).

Studies of cell and organelle integrity by light microscopy and transmission electron microscopy (TEM)

To investigate effects of gamma irradiation on cell and organelle integrity in stem cell aggregates at the end of gamma irradiation and selected post-irradiation time points during the proliferation (5 and 7 weeks) and maturation (11, 15, 17, 20 and 24 weeks) stages, samples were harvested for histological and cytological studies. For each dose rate and developmental stage, samples from 3 different cell aggregates were harvested, fixed and embedded in LR White resin (London Resin Company) according to Lee et al. (2017). For light microscopy studies, 1 µm thick sections were made from embedded samples using an Ultracut Leica EM UC6 microtome (Leica, Mannheim, Germany), stained with toluidine blue O to visualise the cells and inspected using a light microscope with bright field optics (DM6B, Leica). For cytological observations, LR white-embedded samples were sectioned into 70 nm ultrathin sections, using an Ultracut microtome (Leica EMUC6) and stained with uranyl acetate and lead citrate before examining by TEM (FEI Morgagni 268).

Analysis of cell wall modifications using immunolabeling

To investigate cell wall modifications in response to the gamma irradiation, indirect immunolabeling of cell wall components was performed in a time course as described in Lee et al. (2017) using 3 plants per dose rate. For this purpose, 1 µm-thick LR White sections were obtained as described above. The sections were incubated with primary rat monoclonal antibodies (Table S1), and then with secondary antibodies (anti-rat-IgG, whole molecule) linked to fluorescein isothiocyanate (FITC), following a standard protocol. Afterwards, the sections were washed with PBS buffer, mounted with fluoro-gel (EMS) and examined using a microscope equipped with epifluorescence (Leica DM6B).

RNA extraction

At the end of the gamma irradiation (time point 1 = T1) and 7 weeks thereafter during the post-irradiation cell proliferation period (proliferation stage 2 = P2), 8 and 4 repeated samples per dose rate, respectively, were harvested for RNA isolation by flash-freezing in liquid nitrogen and stored at -80 °C until further analysis. For each dose rate, four of the T1-samples were used for RNA sequencing (RNA-seq), and four T1-samples and four P2-samples were used for RT-qPCR analysis of transcript levels of specific candidate genes.

Total RNA was extracted using the MasterPure Complete DNA and RNA Purification Kit (Epicenter, Madison, WI, USA), following the manufacturer's protocol except that 1–2% polyvinylpyrrolidone (PVP, mw 360 000, Sigma-Aldrich) was added to the extraction buffer and 1,4-dithiothreitol (DTT) was replaced with 3 µl beta-mercaptoethanol. The concentration of PVP was 1% for the T1-samples and 2% for the P2-stage samples due to higher phenolic content. The purified RNA was quantified using a NanoDrop ND-1000 Spectrophotometer (Thermo Fisher Scientific) and the quality was determined by an Agilent 2100 Bioanalyzer (Agilent Technologies).

RNA seq, differential expression analyses and functional term enrichment

The transcriptomes were sequenced on the Illumina HiSeq4000 platform at the Norwegian Sequencing Centre (University of Oslo, Oslo, Norway) using the Strand specific 20 × Truseq RNA library preparation (paired end; with read length of 150 bp) on two lanes on the HiSeq 4000 instrument.

Analyses of the RNA-seq data were performed as described in Bhattacharjee et al. (2025). The transcript

abundances were estimated using the Salmon package (Patro et al. 2017) comparing each dose rate with the Norway spruce genome [*Picea abies* 1.0 assembly, plantgenie.org (Nystedt et al. 2013)]. Gene expression in the different gamma-irradiated samples was compared with the unexposed control samples using DESeq2. Genes were classified as differentially expressed genes (DEGs) if the False Discovery Rate (FDR) (Benjamini & Hochberg correction) adjusted *P*-values were < 0.05.

Gene ontology (GO) annotations of Norway spruce genes as well as spruce to *A. thaliana* orthologs by best sequence matches were downloaded from plantgenie.org (Sundell et al. 2015). Enrichment of GO terms or KEGG (Kyoto Encyclopedia of Genes and Genomes) pathways in sets of DEGs was performed using topGO (version 2.34.0) or kegga from the limma package (version 3.38.2), respectively. The *A. thaliana* orthologs were used to associate the Norway spruce genes with KEGG pathways.

RT-qPCR analysis

For P2 and T1 samples, cDNA was synthesised from 1 µg of RNA in a 20 µl reaction using SuperScript™ VILO™ cDNA Synthesis Kit (Invitrogen) following the manufacturer's protocol and no enzyme controls (-RT) were made for each sample. Eight genes belonging to the functional categories DNA repair and unfolded protein response (UPR) were selected (Table S2) for the RT-qPCR analysis, based on their significant regulation by gamma irradiation as revealed by the RNA-seq analyses. To design primers, gene sequences were retrieved from PlantGenIE (plantgenie.org) (Table S2). Primers were designed using the online tools Oligoanalyzer (eu.idtdna.com/calc/analyzer) and Primer Blast (ncbi.nlm.nih.gov/tools/primer-blast/) with default parameters. All amplifications were performed in a 7500 Fast Real-time PCR system (Applied Biosystems) using 20 µl of Platinum Quantitative PCR Supermix-UDG and SYBRGreen (Thermo Fisher Scientific).

To compare the relative transcript levels of the selected genes in the samples exposed to different dose rates of gamma radiation with the unexposed controls, the comparative C_T (Cycle threshold) method (known as $\Delta\Delta C_T$ method) was used (Livak and Schmittgen 2001). The expression of the target genes was normalised by the mean expression of the three reference genes, *α-TUBULIN*, *ACTIN*, *ELONGATION FACTOR 1α*. Four biological replicates per dose rate with 4 technical replicates of each were used in the qPCR analyses.

Statistical analyses of DNA damage and qPCR gene expression data

For statistical analyses of DNA damage and gene expression analysed by qPCR, one-way analyses of variance (ANOVA) in the general linear model mode, followed by Tukey's post hoc test, was performed ($P \leq 0.05$) using the Minitab statistical software (Minitab 18, Minitab Inc). Prior to these analyses, tests for equal variance and normal distribution were performed using Levene's and Ryan-Joiner's tests, respectively. Due to lack of normal distribution, the gene expression data were log10 transformed prior to the ANOVA (Minitab 18).

Results

No visible effect of gamma irradiation on cell proliferation or subsequent embryogenesis

There were no signs of differential proliferation or any other visible changes in the stem cell aggregates for any of the gamma dose rates following the 144-h gamma irradiation (Fig. 1a). Also, during the post-irradiation proliferation and subsequent maturation stages after transfer to embryogenesis-induction media, there were no visible differences between the gamma-exposed and the control cells (Fig. 1a, Fig. S1). Somatic embryos developed post-irradiation regardless of gamma dose rate; equal numbers of embryos were obtained in the controls and at 100 mGy h^{-1} (Fig. S1, Table S3). However, normal embryos with 7–8 cotyledons (Alvarez et al. 2015) were observed in the unexposed control only (results not shown).

Dose rate-dependent DNA damage in gamma-irradiated cells

COMET analyses revealed significant DNA damage at ≥ 10 mGy h^{-1} (Fig. 1b). In response to 10, 20, 40 and 100 mGy h^{-1} the cells showed 5.8, 27.2, 26.3 and 34.9% tail DNA (Fig. 1b). At 100 mGy h^{-1}, the DNA damage level was about 330 times higher than in the control (0.1% tail DNA) and about 10 times higher than at 1 mGy h^{-1} (3.8%).

Gamma radiation-induced cell and organelle damage at all dose rates

Light microscopy (Fig. 2a) and TEM (Fig. 2b) analyses revealed cellular abnormalities such as disintegrating nuclei and nuclear membranes, disarrayed mitochondrial cristae, and accumulation of amorphous materials in the cells at all gamma radiation dose rates at the end of the irradiation as well as during the post-irradiation stages. Generally,

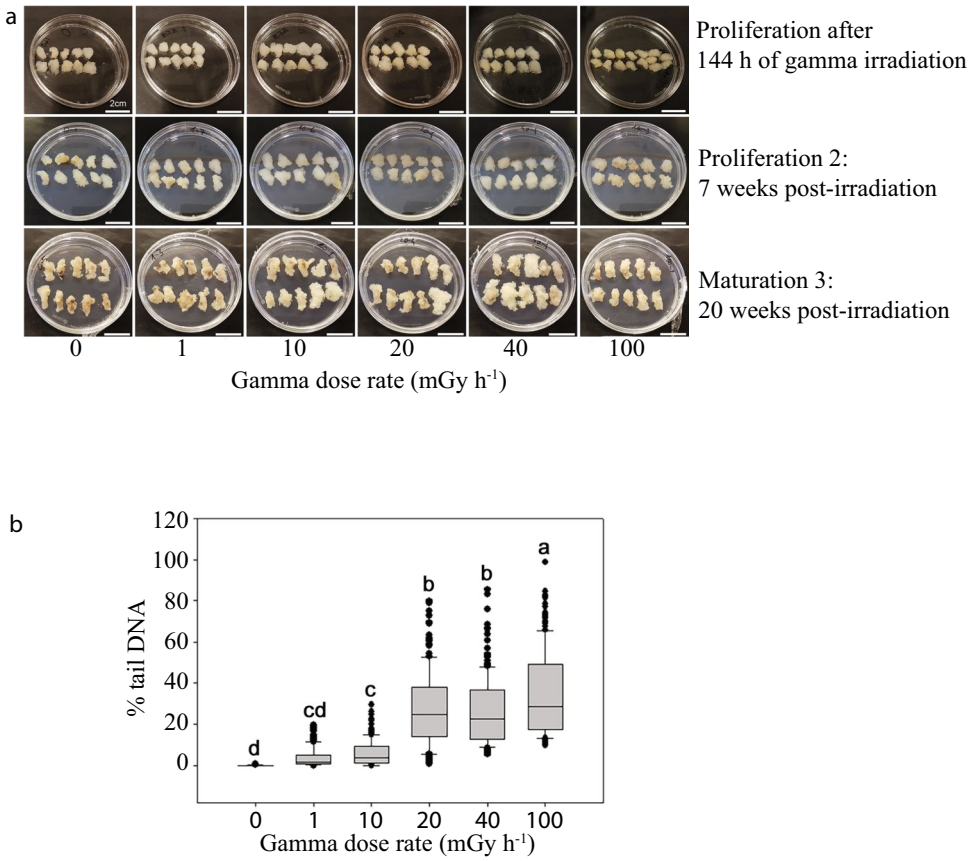

Fig. 1 Effect of 144 h of gamma irradiation on clonal stem cells of Norway spruce. **a** Proliferating stem cell aggregates at the end of the exposure (upper panel) and during post-irradiation stages. Scale bars: 2 cm. **b** DNA damage after the gamma irradiation as measured by the COMET assay. The line in each box represents the median values of 3 biological replicates per dose rate with three technical replicates (gels) for each ($n = 200$ nuclei per gamma dose rate with 60–70 nuclei per biological replicate). Lower and upper boundaries = 25 and 75 percentiles, error bars = 10 and 90 percentiles with data points outside these shown as dots. Different letters indicate significant differences ($p \leq 0.05$) based on analysis of variance followed by Tukey's test

as expected, the cells gradually developed a more compact structure with smaller vacuoles, although exceptions with larger vacuoles were also observed, particularly for gamma-irradiated cells with different cellular abnormalities (Fig. 2a).

Cell wall modifications in response to gamma radiation

At the end of the gamma-irradiation, no immunofluorescence signal was detected for the methyl-esterified homogalacturonan (HG) pectin using the LM20 antibody, and the control cells exhibited a weak signal only (Fig. S2a). However, during the post-irradiation culture period, both the unexposed control and gamma-irradiated cells showed similar, stronger signals. The abundance of un-methyl-esterified HG detected by the LM19 antibody did not differ between the 144 h-gamma-irradiated and control cells, but at the post-irradiation stages (from 7 weeks), the immunofluorescence signal was generally stronger in the gamma-irradiated cells (Fig. S2b). The signal for the hemicellulose xyloglucan detected by the LM15 antibody appeared similar at all gamma radiation dose rates both at the end of the gamma irradiation and post-irradiation, but there were no or very low signals only in the unexposed control cells (Fig. S2c). The arabinogalactan protein detected by the JIM13 antibody was observed in gamma-irradiated cells during late post-irradiation maturation stages only, but not in control cells at any stage (Fig. S2d).

Substantially altered transcriptomes in response to gamma-irradiation

RNA-seq analysis revealed that the number of differentially expressed genes (DEGs) between the gamma-irradiated cells (144 h) and the unexposed controls increased with increasing dose rate (Fig. 3a). Amongst 66,069 predicted genes in Norway spruce, 17,047 (25%) were DEGs (FDR adjusted P-values < 0.05) (Fig. 3b). Although there was a substantial number of unique DEGs for each dose rate, some overlap between the dose rates was observed (Fig. 3c). Moreover, 15,365 genes showed significant difference in expression at 100 mGy h^{-1} compared to the unexposed controls. GO (Fig. S3) and KEGG pathway (Fig. S4) enrichment analyses showed that cell cycle/cell division, DNA repair mechanisms, DNA methylation-dependent chromatin silencing-related genes, and selected pathways involved in development were enriched for DEGs. GO categories related to initiation and regulation of DNA replication, G2/M transition and cell proliferation

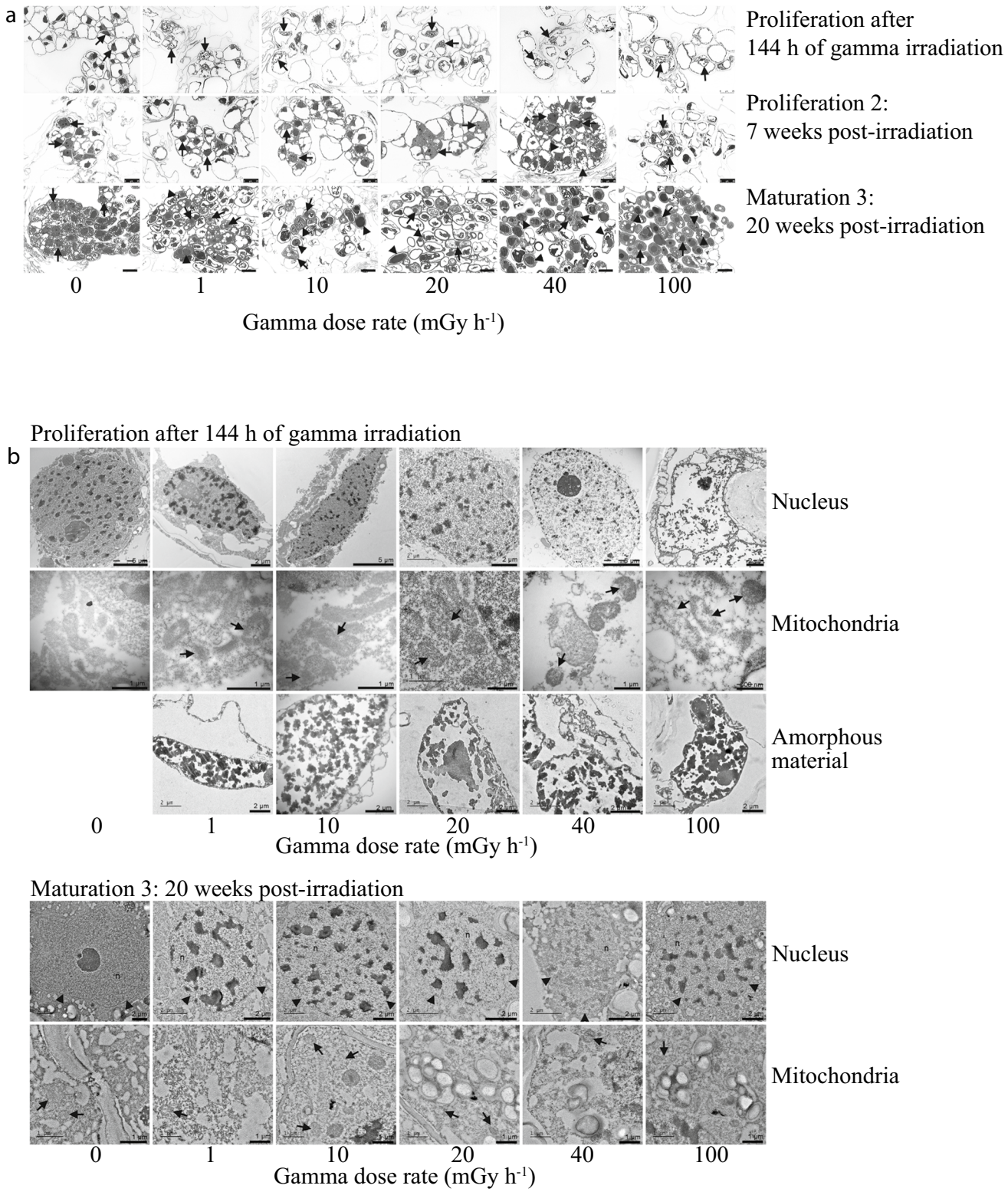

Fig. 2 Cellular damage in clonal stem cells of Norway spruce after 144 h of gamma irradiation. **a** Light micrographs at the end of the exposure (upper panel) and during post-irradiation proliferation and maturation stages (middle and lower panel). Arrows indicate cell nuclei and arrowheads indicate amorphous materials. Scale bars: 25 µm. **b** Transmission electron micrographs of stem cells of Norway spruce at the end of the gamma irradiation (upper three panels) and during a post-irradiation maturation state (lower two panels). Arrows indicate the location of organelles in normal control cells and cellular abnormalities in gamma-exposed cells. Lower panel: n, nucleus; arrowheads (0–10 mGy h^{-1}), intact nuclear envelope; higher doses (20–100 mGy h^{-1}), disintegrating nuclear membranes and nuclei

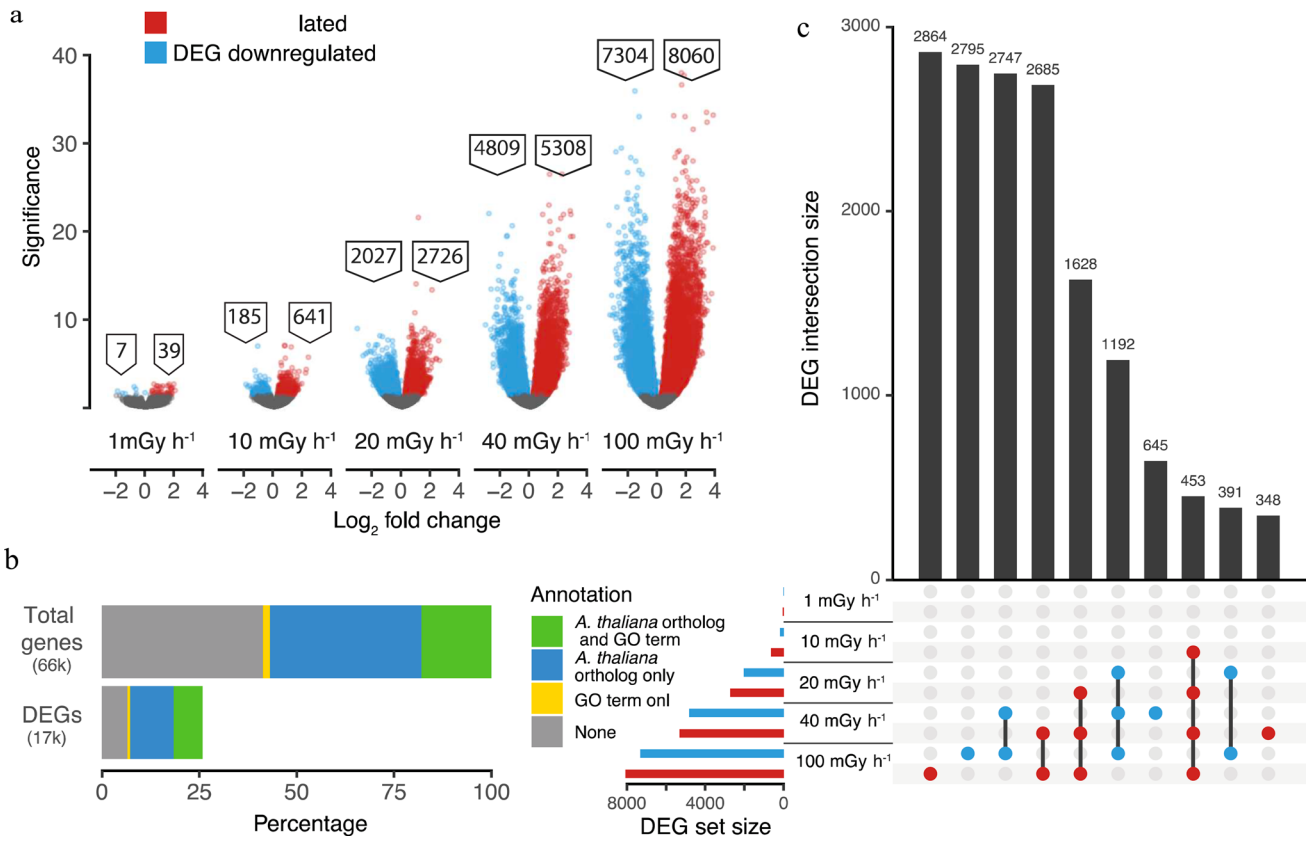

Fig. 3 Effect of different gamma dose rates for 144 h on gene expression in clonal stem cells of Norway spruce. For each dose rate, four repeated samples were analysed in duplicate by RNA sequencing. **a** Number of differentially expressed genes (DEGs; $\log_2$ fold change in DEGs, adjusted *P*-value < 0.05) with up- (red) or down- (blue) regulated genes relative to the unexposed control (0 mGy h^{-1}). **b** Percentages of the total number of genes and DEGs (25% of the total) with available annotation data (Gene Ontology (GO) terms or an *Arabidopsis thaliana* gene ortholog). **c** Upset plot showing the numbers of up- (red) or down- (blue) regulated DEGs and overlap between the different gamma dose rates

were enriched for downregulated DEGs (Fig. S3), indicating that regulation of cell cycle and replication must be considerably hindered due to radiation stress. Additionally, KEGG enrichment analyses found DNA repair pathways such as base excision repair, nucleotide excision repair and mismatch repair among the most enriched pathways for downregulated DEGs (Fig. S4). A wide range of genes encoding transcription factors, hormonal pathways, protein folding, protein degradation and transport and secondary cell wall biogenesis also demonstrated modified transcriptional patterns upon the radiation stress (Table 2, 3, 4, 5, 6 and 7, additional information and details in Table S4-S11).

Gamma radiation-induced changes in expression of genes related to antioxidants, DDR, cell cycle regulation and epigenetics

A wide range of antioxidant biosynthesis and signalling genes were significantly regulated in cells exposed to dose rates ≥ 40 mGy h^{-1} (Table 2, Table S4). Among others, a range of *PEROXIDASEs* (*PER*s), *GLUTATHIONE-S-TRANSFERASES* (*GSTU*s) and *PHENYLCOUMARAN BENZYLIC ETHER REDUCTASE 1* (*PCBER1*) showed upregulation mostly at 40–100 mGy h^{-1}. *SUPEROXIDE DISMUTASEs* (*SOD*s), on the other hand, were downregulated at ≥ 40 mGy h^{-1}.

More than 250 DDR-related genes were significantly regulated after the gamma irradiation, with approximately 95% showing downregulation, particularly at 100 mGy h^{-1} (Tables 3, S5). *SUPPRESSOR OF GAMMA RESPONSE 1* (*SOG1*) that encodes a master regulator of DNA damage-induced cell cycle arrest in plants, was downregulated at all dose rates and decreased with increasing dose rate. *RAD4*, *RAD5A*, and *RAD50* were downregulated at 100 mGy h^{-1} (Table 3). The DNA repair protein *X-REPAIR CROSS COMPLEMENTING 3* (*XRCC3*) gene was one of the few DEGs that showed upregulation.

Significant downregulation of cell-cycle related genes was observed at dose rates ≥ 40 mGy h^{-1} (Tables 3, S6). The pro-spindle assembly factor *TARGETING PROTEIN*

Table 2 Differentially expressed antioxidant-related genes in clonal stem cells of Norway spruce after exposure to 144 h of gamma radiation at different dose rates. Red and blue highlights denote upregulation and downregulation, respectively, compared to the unexposed control (0 mGy h^{-1}). More intense colour denotes more up-/downregulation. Green borders denote significant fold changes ($p \leq 0.05$: $n = 4$)

Name	Name abbreviation	Gene Id	Fold change (Log_2) in dose rates (mGy h^{-1})				
			1	10	20	40	100
Superoxide dismutase 3	*FSD3*	MA_864356g0010	-0.34	-0.23	-0.57	-1.16	-2.18
Isoflavone reductase homolog PCBER1	*PCBER1*	MA_201611g0010	0.19	0.53	0.47	1.15	1.70
Isoflavone reductase homolog PCBER1	*PCBER1*	MA_10424g0010	0.68	1.20	1.47	1.84	2.73
Flavone 3'-O-methyltransferase 1	*OMT1*	MA_10430251g0010	-0.60	-1.09	-1.03	-1.47	-1.60
L-ascorbate peroxidase 3	*APX3*	MA_20242g0010	0.03	0.02	0.37	0.44	0.66
Peroxidase 45	*PER45*	MA_10427194g0010	0.91	0.75	0.88	1.86	3.02
Peroxidase	*PER12*	MA_458849g0010	0.17	0.82	0.93	1.77	1.76
Peroxidase	*PER27*	MA_88476g0010	0.98	0.82	0.15	1.57	1.86
Peroxidase	*PER3*	MA_25748g0010	1.09	0.76	0.71	1.56	1.67
Peroxidase	*PER27*	MA_829274g0010	-0.21	-0.62	-1.29	-1.11	-1.49
Peroxidase 11	*PER11*	MA_10431506g0010	1.06	0.57	0.43	1.43	2.01
Peroxidase 49	*PER49*	MA_8977627g0010	0.11	0.13	-0.28	1.24	1.17
Peroxidase 24	*PER24*	MA_10435488g0010	1.11	1.28	1.09	1.65	2.93
Peroxidase 30	*PER30*	MA_186946g0010	0.99	1.26	0.87	1.43	2.57
Peroxidase 63	*PER63*	MA_10431460g0010	0.07	-0.57	-0.39	-0.60	-1.37
Peroxidase 43	*PER43*	MA_10429595g0010	-0.04	0.31	0.64	0.23	1.07
Glutathione S-transferase U18	*GSTU18*	MA_738434g0010	0.79	0.93	0.99	1.41	2.26
Glutathione S-transferase U17	*GSTU17*	MA_584053g0010	0.01	0.52	0.00	0.61	2.06
Glutathione S-transferase U11	*GSTU11*	MA_8443026g0010	0.43	0.37	0.20	0.37	1.51
Glutathione S-transferase U28	*GSTU28*	MA_8564957g0010	-0.68	-0.58	-1.29	-0.99	-1.76
Glutathione S-transferase DHAR2	*DHAR2*	MA_103215g0010	-0.36	-0.32	-1.20	-0.04	-1.41
Glutathione S-transferase U20	*GSTU20*	MA_10250723g0010	0.38	-0.71	-0.70	-1.62	-2.04

Table 3 Differentially expressed DNA repair and cell cycle-related genes in clonal stem cells of Norway spruce after exposure to 144 h of gamma radiation at different dose rates. Red and blue highlights denote upregulation and downregulation, respectively, compared to the unexposed control (0 mGy h^{-1}). More intense colour denotes more up-/downregulation. Green borders denote significant fold changes ($p \leq 0.05$: $n = 4$)

Name	Name abbreviation	Gene Id	Fold change (Log_2) in dose rates (mGy h^{-1})				
			1	10	20	40	100
DNA repair protein RAD50	*RAD50*	MA_10429947g0010	-0.10	0.03	-0.40	-0.20	-0.59
DNA repair protein RAD4	*RAD4*	MA_185929g0010	-0.13	-0.25	-0.35	-0.56	-0.61
DNA repair protein RAD5A	*RAD5*	MA_55086g0010	-0.10	-0.70	-0.94	-1.80	-2.01
DNA repair protein XRCC3 homolog	*XRCC3*	MA_10435430g0020	-0.22	0.09	0.34	0.45	0.60
Protein gamma response 1	*GR1*	MA_50946g0010	-0.02	0.50	0.72	0.95	1.22
SUPPRESSOR OF GAMMA RESPONSE 1	*SOG1*	MA_98008g0010	-0.34	-0.41	-0.39	-1.03	-1.47
Cyclin-dependent kinase B1-2	*CDKB1-2*	MA_325398g0010	-0.09	-0.40	-0.44	-0.76	-1.81
Cyclin-dependent kinase B2-2	*CDKB2-2*	MA_16797g0020	-0.32	-0.31	-0.36	-0.59	-2.09
Protein TPX2	*TPX2*	MA_10430768g0010	-0.13	-0.27	-0.80	-0.75	-2.04
Cyclin-A2-2	*CYCA2-2*	MA_88982g0010	-0.29	-0.68	-1.00	-1.26	-2.48
DNA topoisomerase 2	*TOP2*	MA_6634g0010	-0.21	-0.59	-0.96	-1.11	-2.41
DNA replication licensing factor MCM3	*MCM3*	MA_163650g0010	-0.34	-0.61	-0.88	-1.74	-2.12
DNA replication licensing factor MCM5	*MCM5*	MA_10426777g0010	-0.22	-0.70	-0.83	-1.55	-1.95
Mini-chromosome maintenance (MCM2/3/5) family	*MCM6*	MA_15713g0010	-0.15	-0.54	-0.75	-1.23	-1.75
DNA replication licensing factor MCM7	*MCM7*	MA_10426237g0010	-0.27	-0.67	-0.80	-1.32	-1.80
Structural maintenance of chromosomes protein	*ATSMC3*	MA_317249g0010	-0.35	-0.53	-1.09	-1.27	-2.06

FOR XKLP2 (*TPX2*), *CYCLIN A2* (*CYC2A2*) and the cyclin-dependent kinase genes, *CDKB1* and *CDKB2*, were downregulated at ≥ 40 mGy h^{-1} (Tables 3, S6). *DNA TOPOISOMERASE 2* (*TOP2*) and multiple genes encoding components of the mini-chromosome maintenance protein complex (MCM; a DNA helicase), and *STRUCTURAL MAINTENANCE OF CHROMOSOME 3* (*SMC3*) showed dose-responsive downregulation at ≥ 20 mGy h^{-1} (Table 3).

Table 4 Differentially expressed epigenetics or chromatin modification-related genes in clonal stem cells of Norway spruce after exposure to 144 h of gamma radiation at different dose rates. Red and blue highlights denote upregulation and downregulation, respectively, compared to the unexposed control (0 mGy h^{-1}). More intense colour denotes more up-/downregulation. Green borders denote significant fold changes ($p \leq 0.05$: $n = 4$)

Name	Name abbreviation	Gene Id	Fold change (Log_2) in dose rates (mGy h^{-1})				
			1	10	20	40	100
ATP-dependent DNA helicase DDM1	*DDM1*	MA_42406g0010	-0.54	-0.50	-1.04	-1.19	-2.02
DNA (cytosine-5)-methyltransferase CMT2	*CMT2*	MA_173651g0020	-0.59	-0.69	-1.08	-1.42	-2.34
DNA (cytosine-5)-methyltransferase CMT3	*CMT3*	MA_173651g0010	-0.40	-0.60	-0.83	-1.26	-1.81
Histone chaperone ASF1B	*ASF1B*	MA_73031g0010	-0.39	-0.64	-0.60	-1.48	-1.94
DNA (cytosine-5)-methyltransferase 1	*DMT1*	MA_88843g0010	-0.37	-0.75	-1.02	-1.59	-2.48
Histone H2A	*HTA5*	MA_601125g0010	-0.69	-0.89	-1.32	-0.92	-2.28
HTB11	*HTB11*	MA_454575g0010	-0.74	-0.99	-1.26	-1.92	-2.01
Histone-lysine N-methyltransferase, H3 lysine-9 specific SUVH5	*SUVH5*	MA_790260g0010	-0.79	-0.88	-1.56	-2.25	-2.80
Histone-lysine N-methyltransferase SUVR4	*SUVR4*	MA_106792g0010	-0.26	-0.53	-0.84	-1.51	-1.79
Histone-binding protein MSI1	*MSI1*	MA_10432677g0010	-0.22	-0.69	-0.86	-1.55	-2.17

Table 5 Differentially expressed unfolded protein response (UPR) genes in clonal stem cells of Norway spruce after exposure to 144 h of gamma radiation at different dose rates. Red and blue highlights denote upregulation and downregulation, respectively, compared to the unexposed control (0 mGy h^{-1}). More intense colour denotes more up-/downregulation. Green borders denote significant fold changes ($p \leq 0.05$: $n = 4$)

Name	Name abbreviation	Gene Id	Fold change (Log_2) in dose rates (mGy h^{-1})				
			1	10	20	40	100
E3 ubiquitin-protein ligase UPL2	*UPL2*	MA_10436069g0010	-0.45	-0.43	-1.32	-0.86	-1.52
RBR-type E3 ubiquitin transferase		MA_10053g0010	-0.47	-0.26	-0.96	-1.06	-1.82
MCP2c	*AMC6*	MA_10430487g0010	0.10	0.48	1.13	1.81	2.31
Hsp70-Hsp90 organizing protein 3	*HOP3*	MA_867694g0010	-0.10	-0.33	-0.31	-0.47	-0.92
17.6 kDa class I heat shock protein 3	*HSP17.6C*	MA_10427493g0010	0.66	1.22	1.00	2.77	3.30
HSP21	*HSP21*	MA_10434235g0010	0.22	0.55	1.20	1.74	1.87
Heat shock 70 kDa protein 10, mitochondrial	*HSP70-10*	MA_79699g0010	-0.23	-0.43	-0.26	-1.06	-1.60
Heat shock protein 90-1	*HSP90-1*	MA_10861g0010	0.24	-0.41	-0.30	-0.80	-1.60
HSP90.5	*HSP90-5*	MA_10431770g0010	0.06	-0.24	-0.34	-0.89	-1.34
Heat shock protein 90-6, mitochondrial	*HSP90-6*	MA_82160g0010	-0.14	-0.24	-0.27	-0.77	-1.25
Protein SRC2 homolog	*SRC2*	MA_5321101g0010	-0.16	-0.11	0.52	0.99	1.52
SNARE-like superfamily protein	*YKT61*	MA_252882g0010	-0.01	0.20	0.46	0.83	1.01
Protein SUPPRESSOR OF K(+) TRANSPORT GROWTH DEFECT 1	*SKD1*	MA_465725g0010	0.02	0.20	0.33	0.68	0.78
Vacuolar protein sorting-associated protein 41 homolog	*VPS41*	MA_10436506g0010	-0.28	-0.22	-0.43	-0.53	-0.93

GO terms related to DNA modification were significantly enriched, and nearly 200 genes with predicted function related to epigenetic pathways or chromatin modifications were significantly regulated in a dose rate-dependent manner (Fig. S3, Tables 4, S7). Many genes encoding DNA methylases, helicases, and histone chaperones showed ≥ twofold regulation. The ATP-dependent DNA helicase *DECREASE IN DNA METHYLATION 1* (*DDM1*) gene, *DMT1* (*DEFICIENT IN DNA METHYLATION 1*), *CHROMOMETHYLASE 2 AND 3* (*CMT2* and *CMT3*) were downregulated at ≥ 20 mGy h,$^{-1}$ and one of the histone chaperones *ANTI-SILENCING FACTOR 1B* (*ASF1B)* was downregulated at ≥ 40 mGy h^{-1} (Tables 4, S7). A drastic change in expression of genes encoding the histone 2A (H2A) and 2B (H2B) subunits was also observed, with the H2 component genes *HTA5* and *HTB11* being downregulated at ≥ 10 mGy h^{-1} and at ≥ 20 mGy h^{-1}, respectively (Table 4). In addition, the core histone-binding subunit gene *MULTICOPY SUPPRESSOR OF IRA1* (*MSI1*) and the histone methyltransferase genes *SU(VAR)3–9 HOMOLOGUE 5 (SUVH5)* and *SUVR4* were downregulated from ≥ 20 mGy h^{-1} (Table 4).

Altered expression of UPR and vesicular transport-related genes in response to gamma irradiation

Genes in the UPR pathway showed significantly changed expression (Tables 5, S8). The ER membrane protein

Table 6 Differentially expressed cell wall-related genes in clonal stem cells of Norway spruce after exposure to 144 h of gamma radiation at different dose rates. Red and blue highlights denote upregulation and downregulation, respectively, compared to unexposed control (0 mGy h^{-1}). More intense colour denotes more up-/downregulation. Green borders denote significant fold changes ($p \leq 0.05$: $n = 4$)

Name	Name abbreviation	Gene Id	Fold change (Log_2) in dose rates (mGy h^{-1})				
			1	10	20	40	100
Pectin lyase-like superfamily protein		MA_98717g0010	0.19	0.84	1.13	1.87	2.13
Pectin lyase-like superfamily protein		MA_9165956g0010	0.55	1.46	1.02	1.65	3.20
Probable pectinesterase 53	*PME53*	MA_10428207g0020	0.72	1.07	0.58	2.01	2.90
Pectinesterase 2	*PME2*	MA_84680g0010	0.87	1.09	0.63	1.23	2.44
Pectin acetylesterase 11	*PAE11*	MA_10376612g0010	-0.13	0.50	0.55	1.66	1.69
Pectinesterase inhibitor 9	*PMEI9*	MA_29344g0010	-0.24	0.20	0.58	0.64	0.95
pectin methylesterase PCR fragment F	*ATPMEPCRF*	MA_10332149g0010	0.24	0.45	0.12	2.60	2.36
Pectinesterase		MA_67675g0010	-0.08	-0.24	-0.21	-0.72	-1.24
Pectinesterase 11	*PE11*	MA_7274893g0010	0.41	0.40	0.76	0.97	1.32
pectin methylesterase PCR fragment F	*ATPMEPCRF*	MA_177599g0010	0.05	-0.48	-0.70	-0.16	-1.23
Probable pectinesterase 53	*PME53*	MA_99816g0010	0.15	0.57	1.07	1.71	2.20
Pectinesterase 11	*PE11*	MA_87592g0010	0.62	1.10	1.02	2.33	2.89
Pectinesterase 11	*PE11*	MA_304854g0010	0.49	1.20	0.91	2.31	3.15
Pectinesterase 11	*PE11*	MA_18312g0010	0.67	1.14	0.39	1.39	2.11
pectin methylesterase PCR fragment F	*ATPMEPCRF*	MA_158002g0020	-0.28	0.24	0.03	1.90	1.29
Xyloglucan galactosyltransferase MUR3	*MUR3*	MA_13968g0020	0.11	0.45	0.62	1.21	1.28
Xyloglucan galactosyltransferase MUR3	*MUR3*	MA_100374g0010	0.42	0.37	0.43	1.20	1.83
Xyloglucan galactosyltransferase MUR3	*MUR3*	MA_7543346g0010	-0.11	0.42	-0.05	1.54	1.66
Cellulose synthase	*CESA1*	MA_102060g0010	0.12	0.26	0.31	0.70	0.76
Cellulose synthase-like protein E1	*CSLE1*	MA_195271g0010	0.81	1.42	1.06	0.46	2.13
Cellulose synthase	*CESA1*	MA_10430668g0010	-0.09	-0.45	-0.48	-0.94	-1.17
Cellulose synthase	*CESA8*	MA_8216532g0010	0.69	1.12	0.87	0.08	1.40

Table 7 Differentially expressed hormone biosynthesis and signalling genes in clonal stem cells of Norway spruce after exposure to 144 h of gamma radiation at different dose rates. Red and blue highlights denote upregulation and downregulation, respectively, compared to the unexposed control (0 mGy h^{-1}). More intense colour denotes more up-/downregulation. Green borders denote significant fold changes ($p \leq 0.05$: $n = 4$)

Name	Name abbreviation	Gene Id	Fold change (Log_2) in dose rates (mGy h^{-1})				
			1	10	20	40	100
Auxin response factor 16	*ARF16*	MA_2421g0010	-0.07	0.51	0.74	1.55	1.98
Auxin response factor 6	*ARF6*	MA_73460g0010	0.06	0.17	0.34	0.63	0.94
Auxin-responsive protein IAA13	*IAA13*	MA_84793g0010	0.41	-0.49	-0.46	-1.27	-2.21
Auxin-responsive protein IAA26	*IAA26*	MA_123046g0010	-0.04	-0.66	-1.10	-1.83	-2.34
Auxin-responsive protein IAA33	*IAA33*	MA_9357208g0010	0.33	0.63	1.07	1.98	2.14
WAV6	*PIN2*	MA_61553g0020	0.23	-0.40	-0.22	-0.73	-1.11
Auxin efflux carrier component 3	*PIN3*	MA_61553g0010	0.01	-0.56	-0.18	-0.83	-0.86
Auxin-responsive protein SAUR32	*SAUR32*	MA_5864g0010	0.77	1.39	1.11	1.53	3.17
Auxin-responsive GH3 family protein	*JAR1*	MA_376158g0010	-0.34	1.35	1.18	1.48	1.82
Cytokinin dehydrogenase 5	*CKX5*	MA_10433485g0010	-0.54	-1.11	-1.96	-1.96	-2.95
Cytokinin hydroxylase	*CYP735A2*	MA_9176g0010	0.11	-0.66	0.32	-0.88	-1.76
Ethylene-responsive transcription factor ERF013	*ERF013*	MA_3758g0010	0.39	0.46	0.74	1.46	2.04
Ethylene-responsive transcription factor ERF053	*ERF053*	MA_2446g0010	0.24	0.32	0.81	0.94	1.89
Ethylene-responsive transcription factor 1A	*ERF1A*	MA_27309g0010	0.37	0.80	0.26	1.05	2.00
Ethylene-responsive transcription factor 4	*ERF4*	MA_81029g0010	-0.11	0.12	0.11	0.89	1.14
Ethylene-responsive transcription factor RAP2-11	*RAP2-11*	MA_65190g0010	0.07	0.55	0.82	1.70	1.90
Ethylene-responsive transcription factor ESR2	*ESR2*	MA_77420g0010	-0.69	-0.79	-1.28	-1.77	-2.29
Ethylene-responsive transcription factor ERF055	*ERF055*	MA_2040g0010	-1.07	-0.94	-1.39	-1.46	-1.62
KS1	*GA2*	MA_57103g0010	-0.06	-0.83	-1.25	-2.27	-2.82
Gibberellin 20 oxidase 2	*GA20OX2*	MA_281894g0010	0.44	0.03	-0.52	-1.60	-2.42

gene *SRC2*, *YKT61,* a core component of the membrane fusion machinery SNARE complex, were upregulated at ≥ 40 mGy h^{-1} and the *Arabidopsis* type II metacaspase homolog *AMC6* was upregulated at ≥ 20 mGy h^{-1}. Additionally, small HSPs genes (*sHSP*s), such as *HSP17.6c* and *HSP21*, were upregulated even at ≥ 10 mGy h^{-1}

and ≥ 20 mGy h^{-1}, respectively. On the other hand, *VACUOLAR PROTEIN SORTING 41* (*VPS41*) being essential for vacuole biogenesis and fusion, and several genes encoding heat shock proteins (*HSP*s) such as *HSP70* and *HSP90,* were downregulated at ≥ 40 mGy h^{-1}. Moreover, the E3 ubiquitin-protein ligase UPL2 and RBR-type E3 ubiquitin transferase transcripts were downregulated along with many other proteasome components (Tables 5, S8).

Gamma radiation-induced altered expression of cell wall and hormone-related genes

Many cell wall-related genes were significantly regulated in response to the gamma irradiation (Tables 6, S9). Pectin acetylesterase, pectin methylesterase, pectin lyase, and pectin esterase-encoding genes related to cell wall modifications, as well as the xyloglucan galactosyltransferase *MUR3* and the cellulose synthase gene *CESA8,* were mostly upregulated at 40–100 mGy h^{-1}. The cellulose synthase gene *CSLE1* was upregulated at 100 mGy h^{-1} (Tables 6, S9).

Also, significant enrichment of GO terms related to hormone biosynthesis and signalling was observed (Tables 7, S10). Most DEGs in jasmonic acid biosynthetic process, response to jasmonic acid, salicylic acid-mediated signalling pathway, and auxin efflux showed significant regulation from 40 mGy h^{-1}, but a few genes even at ≥ 10 mGy h^{-1} (Tables 7, S10). DEGs encoding auxin-responsive factors (ARFs), such as *ARF16*, *ARF6*, and *JAR1*, an auxin-responsive GH3 family protein, and the early auxin-responsive protein *SMALL AUXIN UP RNA 32* (*SAUR32*) were upregulated at ≥ 10 mGy h^{-1} whereas other auxin response and transport genes, *IAA13*, *IAA26*, *PIN2*, and *PIN3*, were downregulated at ≥ 40 mGy h^{-1} (Tables 7, S10). Genes encoding ethylene-responsive transcription factors, such as *ERF53, ERF1A*, *ERF4*, and *RELATED TO AP2-11* (*RAP2-11*), showed upregulation at ≥ 40 mGy h^{-1}, whereas *ERF013* showed upregulation at ≥ 20 mGy h^{-1}. The cytokinin-biosynthesis gene *CYTOKININ HYDROXYLASE*, the cytokinin degradation gene *CYTOKININ DEHYDROGENASE* 5 (*CKX5*), and the gibberellin (GA) biosynthesis genes *ENT-KARURENE SYNTHASE* (*GA2*) and *GIBBERELLIN 20-OXIDASE 2* (*GA20OX2*) were all downregulated at ≥ 40 mGy h^{-1}.

Post-irradiation expression of selected DNA repair and UPR-related genes

To assess how gamma radiation-regulated DDR- and UPR-related genes were affected post-irradiation, the expression of selected genes at the end of the irradiation (T1) and in a subsequent proliferation (P2) stage was analysed by qPCR (Fig. 4). Whereas *RAD5* and *SOG1* showed a gamma dose rate-dependent expression at T1, with significant downregulation at 40–100 mGy h^{-1}, no significant difference from the unexposed control was observed in P2. Expression of *RAD50, GR1* and *XRCC3* showed much variation at both stages with no clear dose rate-dependent effect. UPR-related genes exhibited significant dose rate-dependent effects mostly at T1 but generally not in P2. Of these genes, *HSP70* and *HSP90* were significantly downregulated at 40–100 mGy h^{-1} at T1 and *HSP90* was significantly upregulated at all dose rates in P2, up to fourfold compared to T1. *RBRE3* was significantly downregulated at ≥ 20 mGy h^{-1} at T1 but no dose-dependent effect was observed in P2.

Discussion

Adverse effects of ionising radiation on plant growth and development, including damage to the SAM-harbouring shoot tips in radiation-vulnerable conifers, are well known (Caplin and Wiley 2018 and references therein; Blagojevic et al. 2019a). Despite the significance of the stem cells of the SAMs for growth, reproduction, and survival of plants, detailed molecular effects of ionising radiation on such stem cells are virtually unexplored. Here we employed in vitro-grown clonal stem cells of Norway spruce to assess the effect of gamma radiation on their proliferation and stemness, as well as to characterise such cells as a model to investigate molecular toxicity of gamma radiation in ecologically and economically important conifers.

Although no visible damage or reduced cell proliferation of the stem cells was observed after 144 h of gamma irradiation or during the post-irradiation period, damage to DNA, nuclei and mitochondria as well as accumulation of amorphous materials in cells at all dose rates (Figs. 1, 2, S1) demonstrate profound adverse cellular effects. Differences in the abundance of specific cell wall components between gamma-irradiated and control cells also suggest ionising radiation-induced cell wall modifications (Fig. S2). The lack of detection of methyl-esterified homogalacturonan (HG) pectin at the end of the gamma irradiation and higher abundance of un-methyl-esterified HG post-irradiation compared to in unexposed control cells are consistent with the previously reported stress-induced de-methyl-esterification (Lee et al. 2017; Novaković et al. 2018; Rui and Dinneny 2020). Also, the detection of xyloglucan and arabinogalactan protein in gamma-irradiated cells only is in line with previously reported changes in the hemicellulose fraction and induction of arabinogalactan protein in response to abiotic stress (Le Gall et al. 2015). Yet, despite the observed adverse cellular effects, a fraction of the stem cells obviously survived and retained their stemness and accordingly continued to proliferate (Figs. 1a, S1), suggesting mobilisation of repair and protection systems at least to some extent. This at least partly resembles the situation with survival and activation of

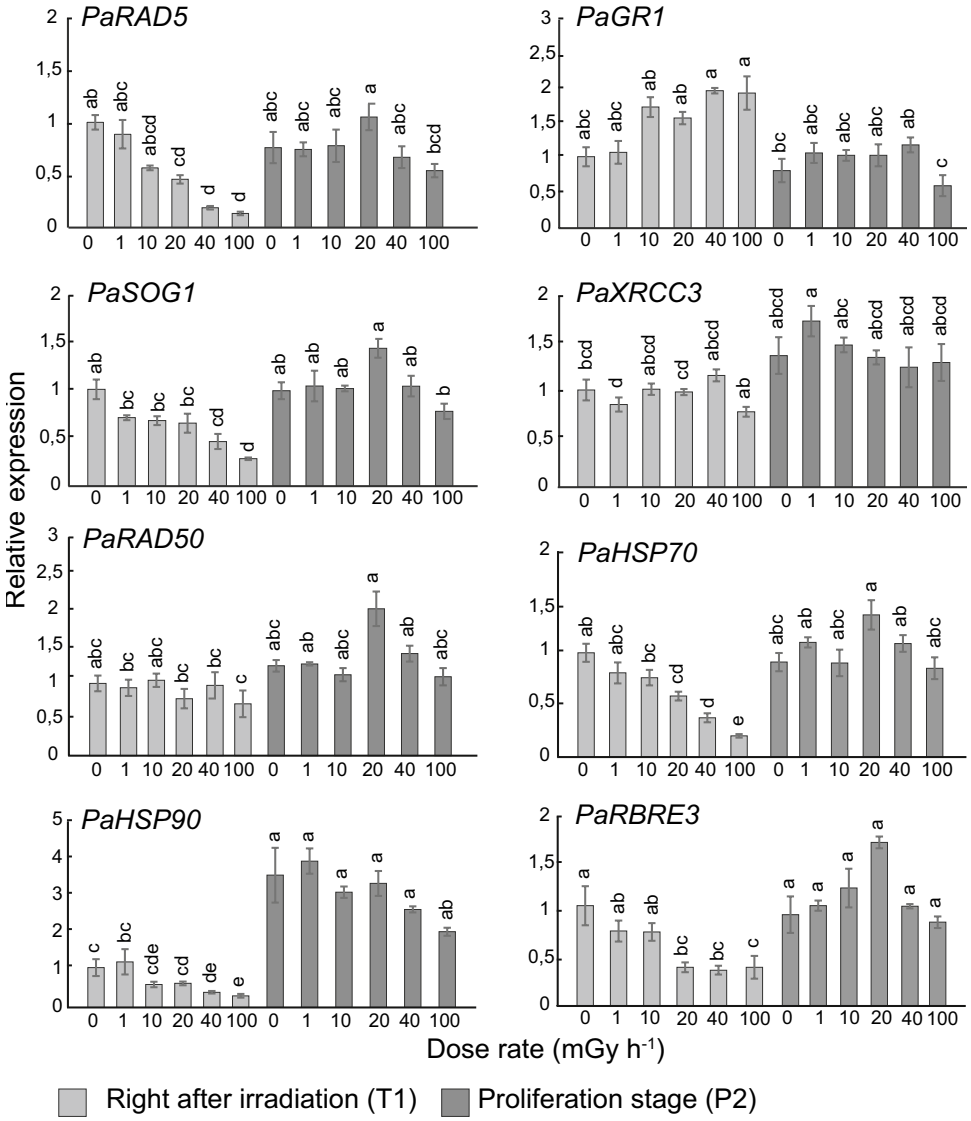

Fig. 4 Relative transcript levels of DNA damage repair (*RAD5*, *GR1*, *SOG1*, *XRCC3*, *RAD50)* and unfolded protein response (UPR; *HSP70*, *HSP90*, *RBRE3*)-related genes after 144 h of gamma irradiation of clonal stem cells of Norway spruce and at 7 weeks post-irradiation (proliferation stage 2). Transcript levels were normalised against *ACTIN*, α-*TUBULIN*, and *ELONGATION FACTOR 1α* and are shown relative to the unexposed controls. The results are mean ± SE ($n = 4$ with 3–4 technical replicates). Different letters within each gene indicate significant difference ($P \leq 0.05$) based on two-way analysis of variance using log-transformed data, followed by Tukey's post-hoc test

axillary meristems despite mortality of the SAM (manifested as lack of apical dominance) in conifers in radionuclide-contaminated areas (Caplin and Wiley 2018; Nybakken et al. 2023).

In addition to direct ionising of vital molecules, gamma irradiation results in ROS accumulation, which can cause persistent damage to macromolecules but also induce protective antioxidant biosynthesis (Sauer et al. 2001; You and Chan 2015). The massive upregulation of antioxidant genes encoding peroxidases, glutathione-s-transferases and lignans (Tables 2, S4) is consistent with this and may at least partly explain the survival of at least a fraction of the stem cells. However, the activity of antioxidants was obviously not sufficient to neutralise the oxidative stress, as judged from the gamma radiation-induced dose rate-dependent DNA and organelle damage. The downregulation of genes encoding SOD (Tables 2, S4) likely contributed to the observed organelle damage. These effects of the 144-h of gamma irradiation on the stem cells of Norway spruce are comparable to observed effects of gamma irradiation of the same duration in Norway spruce and Scots pine seedlings (Blagojevic et al. 2019a) and similar to reported effects of high levels of ionising radiation on other plant species such as *A. thaliana* (Gill and Tuteja 2010; Gill et al. 2015).

Extensive DNA damage is supposed to activate the DDR pathway (Kim et al. 2019). However, in this study, we found overall transcriptional repression of DDR genes, including crucial components of nucleotide excision repair (NER), homologous recombination (HR), replication repair and activation of cell cycle checkpoints (Table 3, Tables S5, S6), suggesting an overall inhibition of the DNA repair consistent with the observed DNA damage in the stem cells (Fig. 1b). In *A. thaliana* plants, cell cycle arrest through a SOG1 and ATM/ATR-dependent DDR pathway is a well-known indicator of DNA damage (Yoshiyama et al. 2014; Kim et al. 2019). Hence, the transcriptional repression of

SOG1 from the lowest dose rates and dose rate-dependent downregulation of cyclins and CDKs (Tables 3, S5) in the stem cells in our study imply a negative effect on the cell cycle, with disruption of cell division and DNA replication (Adachi et al. 2011).

The reduced expression of cell division-related genes is consistent with the downregulation of genes related to biosynthesis of cytokinin and gibberellin and a range of auxin-responsive and auxin transport genes, as well as the upregulation of genes encoding stress-related ethylene-responsive transcription factors (Tables 7, S10). However, although biosynthesis of the main cell division-stimulating hormone cytokinin might be compromised in the irradiated proliferating cells, the downregulation of the cytokinin-degradation gene *CKX* and upregulation of the cytokinin-activation gene *LOG* may suggest that stability of active cytokinin was at least partly maintained (Table S10).

Exposure to ionising radiation can cause genomic instability and long-term effects that can be associated with epigenetic mechanisms such as DNA methylation and modifications of histone tails (Merrifield and Kovalchuk 2013; Braszewska-Zalewska et al. 2014). Multifold repression of multiple genes involved in DNA methylation, histone modification, and nucleosome assembly in the gamma-irradiated stem cells (Tables 4, S7) suggests altered DNA methylation status and modified chromatin dynamics leading to stress-induced genomic instability. Downregulation of *DDM1*, which is involved in DNA repair and methylation, in the stem cells in our study resembles the situation with hypomethylation of DNA and accumulation of DNA damage in UV-B-exposed *A. thaliana* (Müller-Xing et al. 2014). Additionally, the suppression of other genes encoding integral components of the global DNA methylation pathway such as DMT1, CMT2 and CMT3 possibly indicates altered methylation status in the gamma-exposed stem cells compared to the unexposed controls (Feng et al. 2010; Shen et al. 2014). Moreover, since the histone proteins are the building blocks of the nucleosomes, whose synthesis, modification and exchange are required to maintain appropriate transcriptional properties (Zhou et al. 2015), the repression of *HTA5* and *HTB11* expression by several folds in the stem cells indicates that gamma irradiation has a negative effect on the overall synthesis of H2A and H2B (Moreno-Romero et al. 2012; Braszewska-Zalewska et al. 2014; Zhou et al. 2015). This could mean a reduced availability of core histone components affecting chromatin dynamics and transcriptional regulation of genes. However, as H2A modification is also associated with DDR, this downregulation may also have contributed to the ineffective DDR in the gamma-irradiated stem cells.

Upon stress exposure, UPR is induced to cope with misfolded and unfolded proteins in ER by activating molecular chaperons and degradation of misfolded proteins to restore homeostasis (Howell 2013). Activation of UPR-transducers such as bZIP17/28/60, NAC017/062/089/103, and others are crucial in this process (Nawkar et al. 2018). In the gamma-irradiated stem cells, significant upregulation of *bZIP17* (Tables 5, S8) at all dose rates is a direct indication of UPR being a fundamental response in ionising radiation-induced stress. Additionally, genes encoding chaperons such as HSPs in ER and the interaction between HSP90 and the 26 s proteasome machinery are crucial for the assembly and maintenance of the proteasome required for stress-mediated protein folding (Kurepa et al. 2009; Nishizawa-Yokoi et al. 2010). Hence, downregulation of multiple homologs of *HSP*s, *HOP*s, and *E3 LIGASES* from 20 mGy h^{-1} (Table 5) indicates severely compromised protein folding machinery (Mazzucotelli et al. 2006; Peralta et al. 2013; Sharma et al. 2016). Some HSPs also function in coordination with other molecular chaperones and protect misfolded proteins targeted to ATP-dependent refolding or degradation (Bernfur et al. 2017), and are known to provide stress tolerance in *A. thaliana* (Sun et al. 2002). Thus, significant induction of *HSP17.8* and *HSP21* expression in response to gamma radiation (Tables 5, S8) indicates that components of the stress response mechanism involved in the maintenance of the structural integrity of proteins are to some extent in action to provide some protection against gamma radiation-related damage.

Continued stem cell proliferation post-irradiation was consistent with the altered post-irradiation expression (stage P2) of specific DDR- and UPR-related genes (as revealed by RT-qPCR analyses) compared to the end of the gamma-irradiation (stage T1). Whereas the DDR-related genes *RAD51* and *SOG1* and the UPR-related genes *HSP70* and *HSP90* showed downregulation at the T1 stage, no significant regulation of *RAD51* and *SOG1* and upregulation of *HSP90* at the P2 stage imply that the stem cells were able to recover post-irradiation from the radiation-induced transcriptional repression.

Moreover, despite substantial cellular and DNA damage, the surviving stem cells developed somatic embryos at all gamma dose rates during the post-irradiation period following their transfer to maturation media (Fig. S1). Although somatic embryo cultures may commonly generate a proportion of abnormal embryos (Alvarez et al. 2015), the consistent absence of normal cotyledon number (7–8) across all gamma dose rates, unlike in controls, suggests an adverse after-effect of the gamma radiation. The altered expression of genes involved in auxin response and cytokinin metabolism at the end of the gamma irradiation, relative to unexposed controls (Tables 7, S10), may possibly suggest that the subsequent abnormal cotyledon number is, at least partly, radiomorphogenic, resulting from imbalances between cytokinin and auxin. However, it is worth noting that the stem cells were kept on proliferation media with auxin

and cytokinin for 7 weeks post-irradiation before embryo induction on maturation media (containing ABA and IBA), several months later (Fig. S1). This, along with abnormal cotyledon numbers also in some control-derived embryos, suggests that not all deviations can be attributed solely to the gamma irradiation. Nevertheless, the ability of surviving stem cells to undergo embryogenesis at all gamma dose rates post-irradiation implies that these cells had mobilised sufficient repair and protection systems, enabling them to complete embryogenesis, albeit with some abnormalities.

Conclusions

Collectively, the results demonstrate that at least a fraction of the pluripotent stem cells could retain their stemness after exposure to low to moderate levels (1–100 mGy h^{-1} for 144 h) of gamma radiation despite substantial DNA and organelle damage. The RNA-seq analyses revealed massive gamma radiation-induced changes in gene expression towards stress management with upregulation of specific antioxidant genes, protein transport and degradation, but also downregulation of DDR, DNA replication, cell division and protein-folding (UPR) related genes. Yet, the normalisation of the expression of the DDR-related genes *RAD5*, *SOG1* and the UPR-related genes *HSP90*, *HSP70* and *RBRE3* during the post-irradiation proliferation, together with the observed continued cell proliferation and somatic embryo development after transfer to maturation media, demonstrate that the stem cells are able to recover from the gamma radiation-induced stress. Thus, although they sustained extensive damage to an extent that a portion of them died, the surviving cells maintained their stemness and some were capable of embryo formation.

Supplementary Information The online version contains supplementary material available at https://doi.org/10.1007/s00425-025-04819-6.

Acknowledgements Sincere thanks to Tone I. Melby for skilful technical assistance with the RT-qPCR analyses.

Author contributions Payel Bhattacharjee: writing—original draft, writing—review and editing, conceptualisation, investigation, formal analysis, data curation, validation, and visualisation. YeonKyeong Lee: writing—original draft, writing—review and editing, conceptualisation, investigation, formal analysis, data curation, validation, visualisation. Marcos Viejo: writing—review and editing, investigation. Gareth B Gillard: writing—review and editing, data curation, formal analysis. Simen Rød Sandve: writing—review and editing, supervision. Torgeir R Hvidsten: writing—review and editing, supervision. Brit Salbu: writing—review and editing, conceptualisation, funding acquisition, project administration. Dag A Brede: writing—review and editing, conceptualisation, investigation, supervision. Jorunn E. Olsen: writing—original draft, writing—review and editing, conceptualisation, investigation, validation, visualisation, funding acquisition, project administration, supervision.

Funding Open access funding provided by Norwegian University of Life Sciences. This work was supported by funding from the Research Council of Norway through its Centre of Excellence funding scheme (Grant 223268/F50) and from the Norwegian University of Life Sciences.

Data availability The raw RNA sequence data is uploaded in ArrayExpress (accession number E-MTAB-15297). Other data that support the findings of this study are available within the article, in the Supporting Information of this article and in online repositories (gitlab.com/garethgillard/CompRad-Gamma). All data is archived in the Norwegian University of Life Sciences archive (https://dataverse.no/dataverse/nmbu).

Declarations

Conflict of interest The authors declare that there is no conflict of interest.

References

Adachi S, Minamisawa K, Okushima Y, Inagaki S, Yoshiyama K, Kondou Y, Kaminuma E, Kawashima M, Toyoda T, Matsui M, Kurihara D, Matsunaga S, Umeda M (2011) Programmed induction of endoreduplication by DNA double-strand breaks in *Arabidopsis*. Proc Natl Acad Sci USA 108(24):10004–10009. https://doi.org/10.1073/pnas.1103584108

Alvarez JM, Sohlberg J, Engström P, Zhu T, Englund M, Moschou PN, von Arnold S (2015) The *Wuschel-related homeobox 3* gene *Pawox3* regulates lateral organ formation in Norway spruce. New Phytol 208(4):1078–1088. https://doi.org/10.1111/nph.13536

Barescut J, Lariviere D, Stocki T, Vanhoudt N, Cuypers A, Vangronsveld J, Vandenhove H (2011) Study of biological effects and oxidative stress related responses in gamma irradiated *Arabidopsis thaliana* plants. Radioprotection 46(6):S401–S407. https://doi.org/10.1051/radiopro/20116510s

Bernfur K, Rutsdottir G, Emanuelsson C (2017) The chloroplast-localized small heat shock protein Hsp21 associates with the thylakoid membranes in heat-stressed plants. Protein Sci 26:1773–1784. https://doi.org/10.1002/pro.3213

Bhattacharjee P, Blagojevic D, Lee YK, Gillard GB, Grønvold L, Hvidsten TR, Sandve SR, Lind OC, Salbu B, Brede DA, Olsen JE (2025) High radiosensitivity in the conifer Norway spruce (*Picea abies*) due to less comprehensive mobilisation of protection and repair responses compared to the radiotolerant *Arabidopsis thaliana*. Plant Stress 18:101010. https://doi.org/10.1016/j.stress.2025.101010

Blagojevic D, Lee YK, Brede DA, Lind OC, Yakovlev I, Solhaug KA, Fossdal CG, Salbu B, Olsen JE (2019a) Comparative sensitivity to gamma radiation at the organismal, cell and DNA

level in young plants of Norway spruce, Scots pine and *Arabidopsis thaliana*. Planta 250:1567–1590. https://doi.org/10.1007/s00425-019-03250-y

Blagojevic D, Lee YK, Xie L, Brede DA, Nybakken L, Lind OC, Tollefsen KE, Salbu B, Solhaug A, Olsen JE. No evidence of a protective or cumulative negative effect of UV-B on growth inhibition induced by gamma radiation in Scots pine (*Pinus sylvestris*) seedlings. Photochem Photobiol Sci. 2019b;18:1945–1962. https://doi.org/10.1039/c8pp00491a

Braszewska-Zalewska A, Tylikowska M, Kwasniewska J, Szymanowska-Pulka J (2014) Epigenetic chromatin modifications in barley after mutagenic treatment. J Appl Genet 4:449–456. https://doi.org/10.1007/s13353-014-0226-9

Caplin N, Willey N (2018) Ionizing radiation, higher plants, and radioprotection: from acute high doses to chronic low doses. Front Plant Sci 9:847. https://doi.org/10.3389/fpls.2018.00847

Feng S, Cokus SJ, Zhang X, Chen PY, Bostick M, Goll MG, Hetzel J, Jain J, Strauss SH, Halpern ME, Komadu CU, Sadler KC, Pradhan S, Pellegrini M, Jacobsen SE (2010) Conservation and divergence of methylation patterning in plants and animals. Proc Natl Acad Sci USA 107(19):8689–8694. https://doi.org/10.1073/pnas.1002720107

Geras'kin SA, Fesenko SV, Alexakhin RM (2008) Effects of non-human species irradiation after the Chernobyl NPP accident. Environ Int 34(6):880–897. https://doi.org/10.1016/j.envint.2007.12.012

Gichner T, Patková Z, Kim JK (2003) DNA damage measured by the comet assay in eight agronomic plants. Biol Plant 46(2):185–188. https://doi.org/10.1023/B:BIOP.0000022249.86426.2a

Gill SS, Anjum NA, Gill R, Jha M, Tuteja N (2015) DNA damage and repair in plants under ultraviolet and ionizing radiations. Sci World J 2015:250158. https://doi.org/10.1155/2015/250158

Gill SS, Tuteja N (2010) Reactive oxygen species and antioxidant machinery in abiotic stress tolerance in crop plants. Plant Physiol Biochem 48(12):909–930. https://doi.org/10.1016/j.plaphy.2010.08.016

Gupta PK, Durzan DJ (1985) Shoot multiplication from mature trees of Douglas-fir (*Pseudotsuga menziesii*) and sugar pine (*Pinus lambertiana*). Plant Cell Rep 4:177–179. https://doi.org/10.1007/BF00269282

Hansen EL, Lind OC, Oughton DH, Salbu B (2019) A framework for exposure characterization and gamma dosimetry at the nmbu Figaro irradiation facility. Int J Radiat Biol 95:82–89. https://doi.org/10.1080/09553002.2018.1539878

Howell SH (2013) Endoplasmic reticulum stress responses in plants. Annu Rev Plant Biol 64:477–499. https://doi.org/10.1146/annurev-arplant-050312-120053

Johnsen O, Fossdal CG, Nagy N, Molmann J, Daehlen OG, Skroppa T (2005) Climatic adaptation in *Picea abies* progenies is affected by the temperature during zygotic embryogenesis and seed maturation. Plant Cell Environ 28(9):1090–1102. https://doi.org/10.1111/j.1365-3040.2005.01356.x

Kashparova E, Levchuk S, Morozova V, Kashparov V (2020) A dose rate causes no fluctuating asymmetry indexes changes in silver birch (*Betula pendula* (L.) Roth.) leaves and Scots pine (*Pinus sylvestris* L.) needles in the Chernobyl exclusion zone. J Environ Radioact 211:105731. https://doi.org/10.1016/j.jenvrad.2018.05.015

Kim JH, Ryu TH, Lee SS, Lee S, Chung BY (2019) Ionizing radiation manifesting DNA damage response in plants: an overview of DNA damage signaling and repair mechanisms in plants. Plant Sci 278:44–53. https://doi.org/10.1016/j.plantsci.2018.10.013

Koppen G, Azqueta A, Pourrut B, Brunborg G, Collins AR, Langie SAS (2017) The next three decades of the Comet assay: a report of the 11th international comet assay workshop. Mutagenesis 32(3):397–408. https://doi.org/10.1093/mutage/gex002

Kurepa J, Wang S, Li Y, Smalle J (2009) Proteasome regulation, plant growth and stress tolerance. Plant Signal Behav 4(10):924–927. https://doi.org/10.4161/psb.4.10.9469

Kvaalen H, Johnsen O (2008) Timing of bud set in *Picea abies* is regulated by a memory of temperature during zygotic and somatic embryogenesis. New Phytol 177:49–59. https://doi.org/10.1111/j.1469-8137.2007.02222.x

Kvaalen H, Daehlen OG, Rognstad AT, Grønstad B, Egertsdotter U (2005) Somatic embryogenesis for plant production of *Abies lasiocarpa*. Can J for Res 35:1053–1060. https://doi.org/10.1139/x05-035

Le Gall H, Philippe F, Domon J, Gillet F, Pelloux J, Rayon C (2015) Cell wall metabolism in response to abiotic stress. Plants (Basel) 16:112–166. https://doi.org/10.3390/plants4010112

Lee Y, Karunakaran C, Lahlali R, Liu X, Tanino KK, Olsen JE (2017) Photoperiodic regulation of growth-dormancy cycling through induction of multiple bud-shoot barriers preventing water transport into the winter buds of Norway spruce. Front Plant Sci 8:2109. https://doi.org/10.3389/fpls.2017.02109

Lind OC, Oughton DH, Salbu B (2019) The NMBU Figaro low dose irradiation facility. Int J Radiat Biol 95:76–81. https://doi.org/10.1080/09553002.2018.1516906

Livak KJ, Schmittgen TD (2001) Analysis of relative gene expression data using real-time quantitative PCR and the 2(-delta delta C(T)) method. Methods 25:402–408. https://doi.org/10.1006/meth.2001.1262

Mazzucotelli E, Belloni S, Marone D, Leonardis AD, Guerra D, Fonzo ND, Cattivelli L, Mastrangelo A (2006) The E3 ubiquitin ligase gene family in plants: regulation by degradation. Curr Genomics 7(8):509–522

Merrifield M, Kovalchuk O (2013) Epigenetics in radiation biology: a new research frontier. Front Genet 4:40. https://doi.org/10.3389/fgene.2013.00040

Moreno-Romero J, Armengot L, Mar Marquès-Bueno M, Britt A, Carmen Martínez M (2012) CK2-defective Arabidopsis plants exhibit enhanced double-strand break repair rates and reduced survival after exposure to ionizing radiation. Plant J 71:627–638. https://doi.org/10.1111/j.1365-313X.2012.05019.x

Müller-Xing R, Xing Q, Goodrich J (2014) Footprints of the sun: Memory of UV and light stress in plants. Front Plant Sci 5:474. https://doi.org/10.3389/fpls.2014.00474

Nawkar GM, Lee ES, Shelake RM, Park JH, Ryu SW, Kang CH, Lee SY (2018) Activation of the transducers of unfolded protein response in plants. Front Plant Sci 9:214. https://doi.org/10.3389/fpls.2018.00214

Nishizawa-Yokoi A, Tainaka H, Yoshida E, Tamoi M, Yabuta Y, Shigeoka S (2010) The 26S proteasome function and Hsp90 activity involved in the regulation of HsfA2 expression in response to oxidative stress. Plant Cell Physiol 51:486–496. https://doi.org/10.1093/pcp/pcq015

Novaković L, Guo T, Bacic A, Sampathkumar A, Johnson KL (2018) Hitting the wall-sensing and signaling pathways involved in plant cell wall remodeling in response to abiotic stress. Plants 7(4):89. https://doi.org/10.3390/plants7040089

Nybakken L, Lee Y, Brede DA, Mageroy MH, Lind OC, Salbu B, Kashparov V, Olsen JE (2023) Long term effects of ionising radiation in the Chernobyl exclusion zone on DNA integrity and chemical defence systems of Scots pine (*Pinus sylvestris*). Sci Total Environ 904:166844. https://doi.org/10.1016/j.scitotenv.2023.166844

Nystedt B, Street NR, Wetterbom A, Zuccolo A et al (2013) The Norway spruce genome sequence and conifer genome evolution. Nature 497:579–584. https://doi.org/10.1038/nature12211

Patro R, Duggal G, Love MI, Irizarry RA, Kingsford C (2017) Salmon provides fast and bias-aware quantification of transcript

expression. Nat Methods 14:417–419. https://doi.org/10.1038/nmeth.4197
Peralta DA, Araya A, Nardi CF, Busi MV, Gomez-Casati DF (2013) Characterization of the *Arabidopsis thaliana* E3 ubiquitin-ligase *AtSINAL7* and identification of the ubiquitination sites. PLoS ONE 8(8):e73104. https://doi.org/10.1371/journal.pone.0073104
Rui Y, Dinneny JR (2020) A wall with integrity: surveillance and maintenance of the plant cell wall under stress. New Phytol 225(4):1428–1439. https://doi.org/10.1111/nph.16166
Sauer H, Wartenberg M, Hescheler J (2001) Reactive oxygen species as intracellular messengers during cell growth and differentiation. Cell Physiol Biochem 11(4):173–186. https://doi.org/10.1159/000047804
Sharma B, Joshi D, Yadav PK, Gupta AK, Bhatt TK (2016) Role of ubiquitin-mediated degradation system in plant biology. Front Plant Sci 7:806. https://doi.org/10.3389/fpls.2016.00806
Shen X, De Jonge J, Forsberg SK, Pettersson ME, Sheng Z, Hennig L, Carlborg Ö (2014) Natural *CMT2* variation is associated with genome-wide methylation changes and temperature seasonality. PLoS Genet 10(12):e1004842. https://doi.org/10.1371/journal.pgen.1004842
Sparrow AH, Miksche JP (1961) Correlation of nuclear volume and DNA content with higher plant tolerance to chronic radiation. Science 134(3474):282–283. https://doi.org/10.1126/science.134.3474.282
Sun W, Van Montagu M, Verbruggen N (2002) Small heat shock proteins and stress tolerance in plants. Biochim Biophys Acta 1577:1–9. https://doi.org/10.1016/s0167-4781(02)00417-7
Sundell D, Mannapperuma C, Netotea S, Delhomme N, Lin YC, Sjödin A, Van de Peer Y, Jansson S, Hvidsten TR, Street NR (2015) The plant genome integrative explorer resource: Plantgenie. Org New Phytol 208(4):1149–1156. https://doi.org/10.1111/nph.13557
Tenhaken R (2014) Cell wall remodeling under abiotic stress. Front Plant Sci 5:771. https://doi.org/10.3389/fpls.2014.00771
Umeda M, Ikeuchi M, Ishikawa M, Ito T, Nishihama R, Kyozuka J, Torii KU, Satake A, Goshima G, Sakakibara H (2021) Plant stem cell research is uncovering the secrets of longevity and persistent growth. Plant J 106(2):326–335. https://doi.org/10.1111/tpj.15184
Varis S, Klimaszewska K, Aronen T (2018) Somatic embryogenesis and plant regeneration from primordial shoot explants of *Picea abies* (L.) H. Karst. somatic trees. Front Plant Sci 9:1551. https://doi.org/10.3389/fpls.2018.01551
Watanabe Y, Ichikawa S, Kubota M, Hoshino J, Kubota Y, Maruyama K, Fuma S, Kawaguchi I, Yoschenko VI, Yoshida S (2015) Morphological defects in native Japanese fir trees around the Fukushima Daiichi Nuclear Power Plant. Sci Rep 5:13232. https://doi.org/10.1038/srep13232
Yakovlev IA, Lee YK, Rotter B, Olsen JE, Skrøppa T, Johnsen Ø, Fossdal CG (2014) Temperature-dependent differential transcriptomes during formation of an epigenetic memory in Norway spruce embryogenesis. Tree Genet Genomes 10:355–366
Yoschenko V, Nanba K, Yoshida S, Watanabe Y, Takase T, Sato N, Keitoku K (2016) Morphological abnormalities in Japanese red pine (*Pinus densiflora*) at the territories contaminated as a result of the accident at Fukushima Dai-Ichi Nuclear Power Plant. J Environ Radioact 165:60–67. https://doi.org/10.1016/j.jenvrad.2016.09.006
Yoshiyama KO, Kimura S, Maki H, Britt AB, Umeda M (2014) The role of SOG1, a plant-specific transcriptional regulator, in the DNA damage response. Plant Signal Behav 9(4):e28889. https://doi.org/10.4161/psb.28889
You J, Chan Z (2015) ROS regulation during abiotic stress responses in crop plants. Front Plant Sci 6:1092. https://doi.org/10.3389/fpls.2015.01092
Zhou W, Zhu Y, Dong A, Shen WH (2015) Histone H2A/H2B chaperones: from molecules to chromatin-based functions in plant growth and development. Plant J 83:78–95. https://doi.org/10.1111/tpj.12830